PERIODICUM BIOLOGORUM
VOL. 113, No 4, 407–416, 2011

UDC 57:61
CODEN PDBIAD
ISSN 0031-5362

Original scientific paper

4D thermal imaging system for medical applications

KAROLJ SKALA
TOMISLAV LIPIĆ
IVAN SOVIĆ
LUKO GJENERO
IVAN GRUBIŠIĆ

Ruđer Bošković Institute
Centre for Informatics and Computing,
Bijenička 54, HR-10000, Zagreb, Croatia

Correspondence:
Karolj Skala
Ruđer Bošković Institute
Centre for Informatics and Computing,
Bijenička 54, HR-10000, Zagreb, Croatia
E-mail: karolj.skala@irb.hr

Received October 24, 2011.

Abstract

The dissipation of thermal radiation can be observed using thermal infrared cameras which generate images based on the amount of input radiation belonging to a small part of the electromagnetic spectrum (with wavelengths from 7 μm to 15 μm). Since thermal imaging is a simple, contactless, non-invasive and inexpensive imaging method, it is widely applicable in industry, medicine and research. The most common type of thermal imaging involves taking and analyzing only a single thermal image, and it is thus called static thermal imaging. In cases when a thermal process cannot be approximated as static, dynamic thermal imaging and analysis are applied. The idea of combining thermal imaging with 3D scanning methods has spawned in the last few years. 3D thermal imaging can have many applications and purposes, ranging from thermogram rectification to the creation of standardized 3D thermal models of various subjects that can later be used for comparison and evaluation. Although 3D thermal imaging systems exist, all of the examined ones were targeted on the acquisition and analysis of static 3D thermal models.

This paper presents the development of a 4D thermography system through integration of dynamic 3D scanning and thermographic imaging, additionally providing markerless motion analysis, which together enable practical, non-invasive, accurate and automatic monitoring of the temperature changes in the human body, and the characterization of human motion. The workflow of the designed concept is outlined, and the components of the constructed system are thoroughly explained. The process of calibration of the system is described, as well as the methods of motion detection and analysis. Great emphasis is given on the possible medical applications of a 4D thermography system, such as medical diagnostics, human locomotive system rehabilitation and health status monitoring over prolonged time periods.

INTRODUCTION

Temperature distribution on the surface of an object can be determined using a method called *thermal imaging*, often also referenced as *thermography*. It is an imaging technology which is contactless and completely non-invasive. Thermal imaging relies on the principle that all bodies at temperatures higher than 0 K (≈ –273.15 °C) emit electromagnetic (*EM*) radiation. EM radiation, according to its wavelength, is commonly classified within a particular region of the EM spectrum. Visible light and infrared radiation are two adjacent regions in the EM spectrum with wavelengths from 0.38 μm to 0.78 μm, and 0.78 μm to 1 mm, respectively. The intensity and the distribution of EM

radiation over different wavelengths depend mostly on the temperature of an object and the characteristics of its material *(1)*. Major amount of thermal radiation emitted by an object can be observed in a small part of the infrared spectrum, called the *thermal infrared spectrum* (with wavelengths from 7 μm to 15 μm) *(2)*.

Dissipation of thermal radiation can be observed by means of *thermal infrared* (*IR*) *cameras* (hereafter: *thermal camera*). Thermal cameras generate images representing the distribution of thermal infrared radiation on the surface of objects, and can roughly be divided in two groups: imaging cameras and measurement cameras. The difference between them is that thermal measurement cameras are calibrated by the manufacturer and can be used for temperature measurements, while thermal imaging cameras show only the color map of approximate temperature field *(3)*. This makes imaging cameras cheaper and more often used in applications where relative temperature relations are needed more than exact measurements, for example in night surveillance imaging.

Thermography, as a simple, noncontact, non-invasive and inexpensive imaging method, is widely applicable in a variety of different fields in industry and research. Most applications of thermal imaging perform the investigation in a *passive* manner, which means that the camera observes a scene and detects the thermal radiation emitted by objects *(1)*. If differences between analyzed objects' temperatures and ambient temperature are small, the contrast in the thermal image will be poor. This method is called passive since only the existing temperature distribution of the object scene is analyzed, without imposing an additional heat flow to the object *(1)*. Passive thermography is used for various applications such as municipal waste biogas detection *(4),* thermal monitoring of computer systems *(5)*, or evaluation of tumor development and discrimination of cancer *(6)*. In some cases, for example where no natural temperature differences are present, or if envelopes of objects may be too thick for identification of structural elements beneath the surface, *active* thermography methods are used *(1)*. These methods are based on heating (or, in some cases, cooling) of the surface of the observed object and monitoring the change in temperature through time. The object is usually heated by absorption of radiation, electrical heating, eddy currents or ultrasound. Some of the most important methods of active thermography are the locked-in thermography and pulse thermography *(1)*.

Many applications of thermal imaging are based on taking a single image and analyzing the recorded temperature distribution. This method of analysis is called *static thermal imaging*. However, some processes show temperature change rates which cannot be approximated as static. For this purpose, *dynamic thermal imaging* (*DTI*) is applied. DTI monitors, or quantitatively measures, temporal changes in temperature over areas of interest *(2)* . These thermal changes can be monotonic (areas of interest are only warming or cooling), or periodic (manifested as temperature modulation) *(2)*.

Depth cameras are devices designed to provide distance measurement in the form of *depth maps*. A depth map is a 2D array of values where each value represents a distance from the camera to a point in the viewed scene. Although a complex integrated system, a depth camera can, for analysis and calibration, be viewed as a standard RGB camera. Depth values of the captured scene provide the possibility to calculate the point cloud of the scene, and enable reconstruction of the 3D model of that scene. Depth maps can be acquired through any available form of 3D scanning methods, such as laser triangulation, structured light, stereo vision, time-of-flight or holographic interferometry *(7)*. Performance-wise, methods of 3D scanning differ by acquisition rate and computational complexity, influence of ambient light, accuracy, range, cost and other parameters *(7)*. For instance, stereo vision technology is simple, inexpensive and offers high accuracy on well defined targets but is computationally demanding and has low data acquisition rate, while structured light technology enables higher data acquisition rate, but is more complex and expensive.

Besides reconstructing 3D models of a scene from a single point of view, modern real-time depth cameras can be used to develop full 3D scans of objects. An example of such application has been used to create 3D scans of human bodies in home environment with consumer-grade hardware *(8)*. Another interesting utilization of real-time depth cameras is the opening of a whole new range of motion detection and human motion analysis techniques. The knowledge of depth data can significantly influence the complexity and performance of tasks such as body part classification. The afore mentioned problem can, even with the use of inexpensive commodity depth cameras, be performed in real time and enable the estimation of joint positions in the human body *(9)*. With the knowledge of such reference points, markerless motion analysis techniques can be applied relatively easily, creating a new field of research with great potential in the development of medical diagnosis, human motor system rehabilitation or movement analysis for entertainment industry.

Recently, the idea of combining a 3D scanner with thermal imaging (or measurement) technology has started to become more popular *(10–13)*. All systems in the above mentioned references focused on designing 3D thermal imaging systems capable of capturing and analyzing static 3D thermograms. Some important capabilities provided by 3D thermal imaging include the possibilities of thermogram rectification caused by surface emissivity properties, and the creation of standardized thermograms of observed objects for reproducibility and future comparison purposes *(12)*. In this paper, the development and possible medical applications of a novel dynamic passive 3D thermal imaging system are presented, for which we propose a shorter name of *4D thermography* system, where three dimensions represent geometric data in the 3D space and the fourth dimension is time. The main contribution of this system is the utiliza-

tion of the time component, providing the possibilities of more complex, dynamic analyses.

The system combines all capabilities of 3D thermography and human motion capturing and analysis, providing a valuable tool for various medical applications. Integrating different acquisition modalities, it represents a step towards modelling subject-specific human body models that depict subject's anatomy, biomechanics and physiological information from temperature distribution. 4D human models could be used to augment the accuracy of medical diagnosis and enhance monitoring of human health status for rehabilitative or injury prevention purposes.

Next section presents the workflow and the design components of the developed system, as well as giving an overview of its calibration procedure and motion analysis. In section three, possible medical applications of the 4D thermography system are discussed in detail, while section four concludes this paper.

4D THERMOGRAPHIC IMAGING SYSTEM

This section presents the conceptual architecture of the developed system and the methods used for its development. The system architecture is composed of hardware and software components, encompassed by the system workflow. As main components of the system's functionality, calibration process and motion capturing and analysis are described.

System workflow

The concept of the system workflow is based on the conceptual model presented in our previous paper *(11)*. Workflow was expanded and modified to allow for the integration of several imaging and acquisition modalities and enhanced data processing for the purpose of health status monitoring. Compared to the workflow in *(11)*, Figure 1 presents its modification and specialization for dynamic monitoring of the 3D thermal distribution on the surface of objects. The modification of the workflow is denoted by the dashed lines, extending the steps between the acquisition process and medical applications.

The system workflow starts with the calibration process of system components which enables the integration of implemented imaging modalities into a complete dynamic 3D thermal monitoring system. Separate system acquisition devices have to be mutually calibrated with respect to their spatial relations and internal parameters related to their physical properties. Calibration process is described in detail in the next section.

Acquisition process encompasses the simultaneous capturing of data from the calibrated system components that cover the RGB, depth and thermal imaging modalities. The acquisition process has to be performed in a way to enable the real-time processing of the captured data, providing 3D model reconstruction from captured depth maps, motion analysis, skeleton and body part detection, as well as other processing tasks.

The reconstructed real-time 3D model combined with thermal imaging results in a 4D thermal model. 4D thermography allows for a wide number of applications, such as industrial monitoring of processes, construction of autonomous robots and medical applications. This system focuses especially on health status monitoring for the purposes of motor system rehabilitation, dynamic activity tracking, injury prevention and others.

System components

The developed system consists of two main components: hardware, incorporating four different imaging modalities, and software which enables the calibration and functionality of the whole system. Implemented imaging modalities include: a thermal measurement camera, a thermal imaging camera, a RGB camera and a

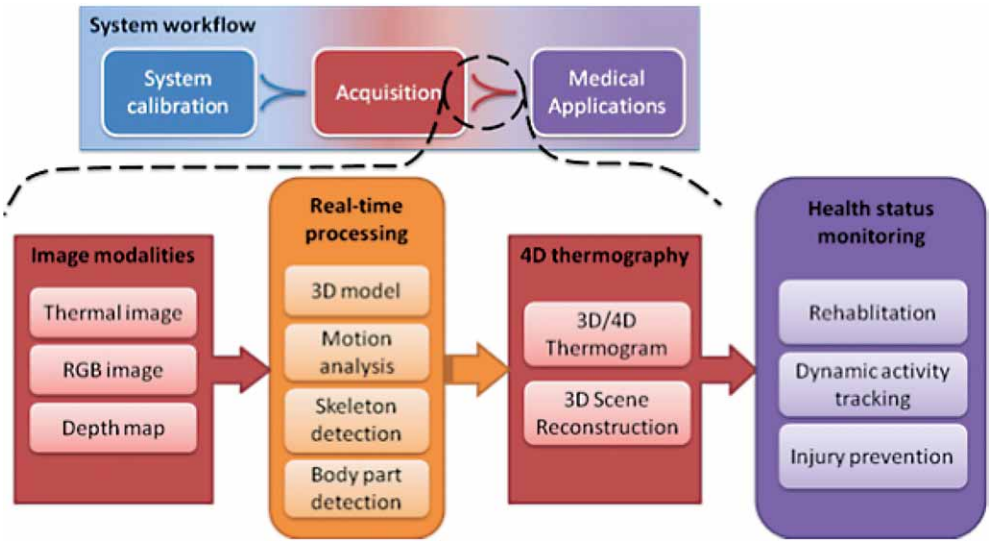

Figure 1. *Workflow of the 4D thermal imaging system.*

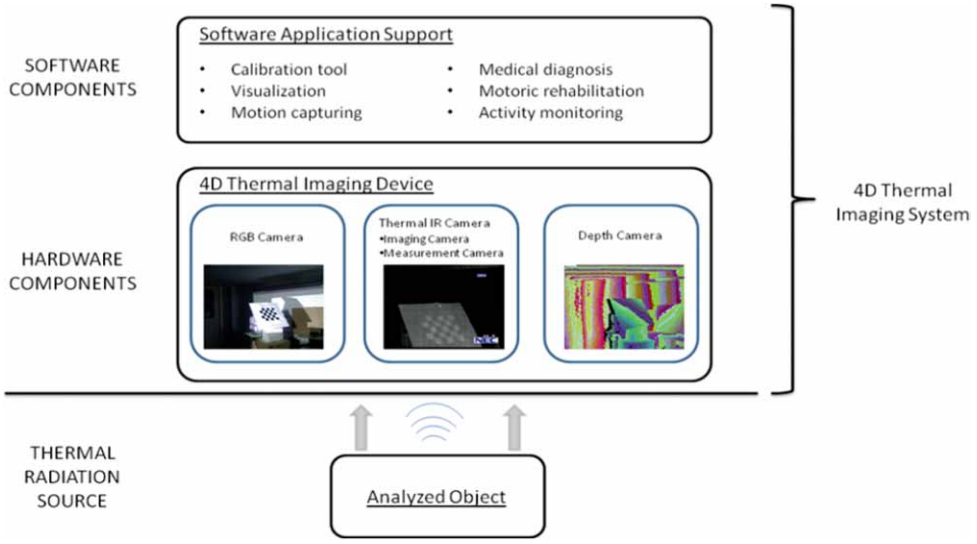

Figure 2. *Components of the developed system.*

depth camera. The structure of the system is presented schematically in Figure 2.

Physical components have been mounted on a single rack, as shown in Figure 3. The depth camera used in construction of the system described in this study is based on the *Microsoft Kinect* device. Its low price and satisfactory measurement accuracy created many interesting new applications and caused Kinect to gain much popularity, not only in the entertainment, but also in the scientific community. Kinect consists of a near-infrared (*NIR*) projector, NIR camera, RGB camera and four microphones firmly mounted together. NIR projector and camera paired together make the depth camera, where the projector emits structured light pattern visible to the NIR camera. The recorded distribution of the pattern in the surrounding environment is then analyzed within Kinect to estimate the depth at each pixel of the captured NIR image. The RGB camera provided with Kinect is the one used in the development of the system, and shown in Figure 2 and Figure 3. The four microphones, although present in the hardware construction of the system, haven't been utilized during the work on this project. Kinect is capable of producing output at the rates of 30 frames per second at the resolution of 640x480 pixels, with the cost that is about fifty times cheaper than a time-of-flight (TOF) camera *(14)*. The effective range of Kinect's depth camera spans from about 0.7 m to 6 m. Aside from low cost, high frame rate and satisfactory imaging quality, other great advantages of Kinect are in the already implemented processing methods. Besides filtering and preprocessing depth maps, Kinect analyzes every captured scene and determines if a person is present in the scene. If so, Kinect estimates the positions of the person's joints, and connects them into a simple skeleton model of the person.

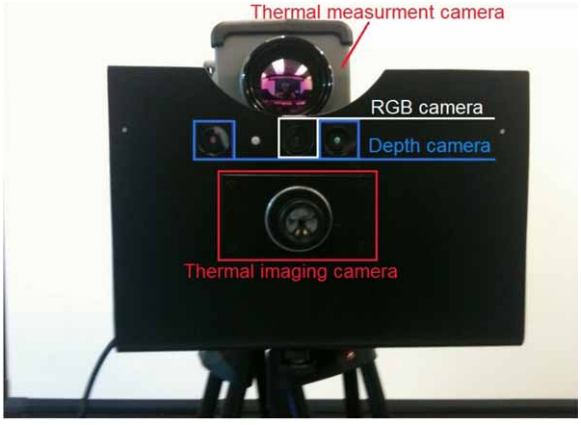

Figure 3. *Constructed 4D thermal imaging system.*

The basic difference between thermal measurement camera and thermal imaging camera has been presented in Introduction. From that of standard RGB cameras. The principle of operation of thermal cameras is slightly different. The process of image acquisition in the thermal EM spectrum is commonly performed in one of two ways: using cooled detectors (containing a refrigerator unit), and non-cooled detectors that operate in the ambient temperature *(3)*. Originally, all thermal imagers had detectors that were cooled to temperatures from –70°C (rarely) to –200°C (most frequently) to stabilize the detector and provide good sensitivity in detection of the energy emitted by objects. Since the introduction of the first camera with a microbolometric array (in 1997), detector cooling was no longer necessary *(3)* because non-cooled thermal imagers are electronically stabilized. Although non-cooled cameras are lighter, faster, cheaper and more reliable, cooled cameras provide greater sensitivity. Both thermal cameras used in the construction of our 4D thermal imaging system were non-cooled. The thermal measurement camera was an NEC Thermotracer, model TH7102WL, and the thermal imaging camera was an ULRvision, model TC384.

Software components are divided into internal system components, enabling the functionality of the system,

and the customized applications dedicated to specific medical purposes. Internal software components include the calibration components, 4D thermal model capturing components and motion analysis components. The implementation of internal software components is based on the methods described in the calibration and motion capturing and analysis subsection, while medical applications are presented in the next section.

System calibration

Camera calibration can be performed in several different ways. A widely used pinhole model of a camera for calculating the camera's intrinsic and extrinsic parameters is described in *(15)*. A more general model that can be used for calculating the parameters of two cameras, as well as their spatial relations, called *stereo calibration*, is presented in *(16, 17)*. Another completely different approach, based on range flow estimation is described in *(18)*, where authors have developed a novel multi-modal range flow algorithm which is robust against typical (technology dependant) range estimation artifacts. Calibration of the system described in this work is based on the pinhole camera model extended for stereo calibration of the RGB and thermal cameras with the depth camera, similar to the calibration process described in *(19)*.

The pinhole camera model is a widely used model to mathematically describe the projection of a point in 3D space onto the imaging plane. The center of the pinhole camera is the center of perspective projection and represents the point in which all the rays intersect. This center is taken as the origin of the coordinate system. The line that passes through the center of projection, and spans in the direction of orientation of the camera, is called the *principal* or *optical axis*. The image plane is perpendicular to the principal axis and lies at the distance f (focal length) from the camera center. The intersection of the image plane and the principal axis is called the *principal point*. Figure 4 shows the structure and components of the pinhole camera model, where M is the point in 3D space, $\boldsymbol{m}$ is the perspective projection of a point from $\boldsymbol{M}$ to the 2D principal plane, p is the principal point at the coordinates (u_0, v_0), f the focal length and X, Y and Z the coordinate axes of the camera, with Z aligned to the principal axis.

In homogeneous coordinates, the 3D world point $\mathbf{M}$ can be written as:

$$\tilde{\mathbf{M}} = [X\ Y\ Z\ 1]^{\mathrm{T}}, \tag{1}$$

where X, Y and Z are the position of point $\mathbf{M}$ in 3D space, and the fourth value is the homogeneous coordinate. The 2D perspective projection $\mathbf{m}$ of $\mathbf{M}$ on the image plane can be written as (also in homogeneous coordinates):

$$\tilde{\mathbf{m}} = [u\ v\ 1]^{\mathrm{T}}, \tag{2}$$

where u and v are the position of point $\mathbf{m}$ on the 2D plane, and the third parameter is the homogeneous coordinate. The perspective projection can be written as:

$$s\mathbf{m} = \mathbf{K}[\mathbf{R}\,|\,\mathbf{t}]\,\mathbf{M} \tag{3}$$

where s is a scale factor, $\mathbf{K}$ the matrix of intrinsic parameters, and $[\mathbf{R}\,|\,\mathbf{t}]$ the joint rotation-translation matrix with extrinsic parameters. If the expression (3) is expanded, it becomes:

$$s\begin{bmatrix} u \\ v \\ 1 \end{bmatrix} = \begin{bmatrix} f_x & 0 & u_0 \\ 0 & f_y & v_0 \\ 0 & 0 & 1 \end{bmatrix} \begin{bmatrix} r_{11} & r_{12} & r_{13} & t_1 \\ r_{21} & r_{22} & r_{23} & t_2 \\ r_{31} & r_{32} & r_{33} & t_3 \end{bmatrix} \begin{bmatrix} X \\ Y \\ Z \\ 1 \end{bmatrix} \tag{4}$$

As can be seen in equation (4), the matrix of extrinsic parameters K consists of the principal point (u_0, v_0), the focal length f_x and the scaled focal length $f_y = k f_x$, where k is the aspect ratio of a pixel *(20)*. If pixels of the camera are square, then $f_y = f_x$. The matrix of intrinsic parame-

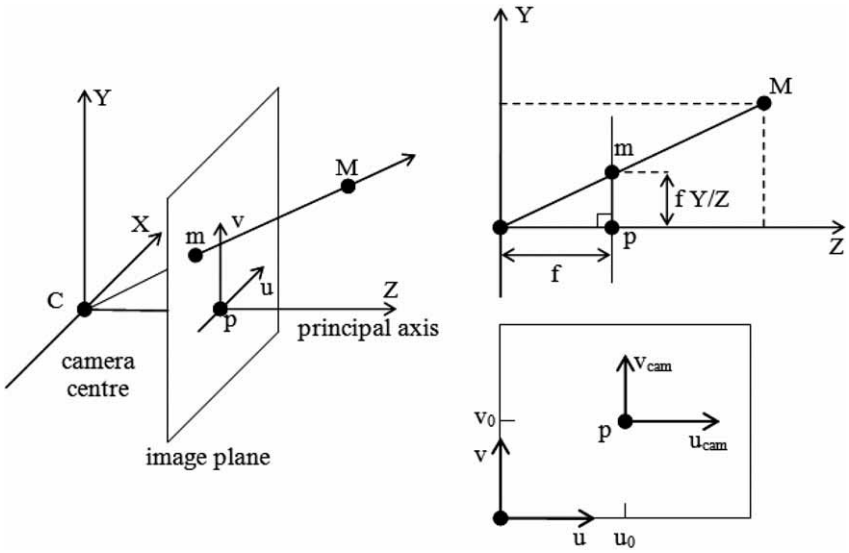

Figure 4. *Schematic presentation of the pinhole camera model.*

ters does not depend on the viewed scene and, once estimated, can be reused if the focal length has been fixed (i.e. in case of zoom lens) *(21)*. In case that the image from the camera has been scaled by some factor, intrinsic parameters also have to be scaled by the same factor. Intrinsic parameters describe the internal parameters of the camera, such as focal distance and radial lens parameters, while the extrinsic parameters indicate the external position and orientation of the camera in the 3D world. To determine the values of intrinsic and extrinsic parameters, a maximum likelihood solution can be found, as shown in *(15)* or *(19)*.

The reverse process of projecting a point from 3D space onto the 2D plane is called back-projection *(22)*. For every 2D image point **m** lying on the plane, there exists an infinite number of 3D world points that can be projected to the same point **m**. All these world points lie on the same line that passes through the camera center and the point **m** on the plane, thus projecting to the same point **m**. Since 2D point **m** reverse maps into this 3D line, it is not possible, because of the lack of information about point-to-camera distance, to use only a RGB or a thermal camera to determine where on that line the original point was located. However, since the pixels of the depth map represent the distance of the object from the camera, this information can be used to back-project the point **m** to the 3D coordinate space. In order to determine the relationship between the depth camera and the RGB and thermal cameras, the depth camera is placed at the origin of the coordinate system:

$$\mathbf{P}_{\downarrow depth} = \mathbf{K}_{\downarrow depth}\,[\mathbf{R}_{\downarrow depth}\,|\,\mathbf{t}_{\downarrow \mathrm{depth}}] = \mathbf{K}_{\downarrow depth}\,[\mathbf{I}\,|\,\mathbf{0}], \quad (5)$$

where $\boldsymbol{P}$ denotes the projection matrix of the camera, $\boldsymbol{I}$ is the identity matrix and $\mathbf{0}$ is the null vector *(20)*. Projection matrix of the RGB camera can be written similarly:

$$\mathbf{P}_{\downarrow RGB} = \mathbf{K}_{\downarrow RGB}\,[\mathbf{R}_{\downarrow RGB}\,|\,\mathbf{t}_{\downarrow RGB}], \quad (6)$$

where $\mathbf{R}_{RGB}$ and $\mathbf{t}_{RGB}$ are the rotation and translation relative to the depth camera. A point **m** (with homogeneous coordinates $\tilde{\mathbf{m}}$) of the depth image can be back-projected into the 3D world as a line that passes through the origin *(20)*:

$$\mathbf{L} = \gamma\, \mathbf{K}_{depth}^{-1}\, \tilde{\mathbf{m}}, \quad (7)$$

for every parameter value γ. If, for every image point, γ is set to be the depth value d of that point, the back-projected point **M** can be calculated:

$$\mathbf{M} = d\, \mathbf{K}_{depth}^{-1}\, \tilde{\mathbf{m}}, \quad (8)$$

Taking the homogeneous coordinates of the 3D point **M**, it can be projected onto the RGB camera:

$$\tilde{\mathbf{m}}_{RGB} = \mathbf{P}_{RGB}\, \tilde{\mathbf{M}}. \quad (9)$$

Calculation of the projection onto the thermal measurement and the thermal imaging camera follows analogously. The calibration process of the system is shown graphically in Figure 5. Detailed accuracy analysis of the calibrated depth and RGB cameras is presented in *(19)*.

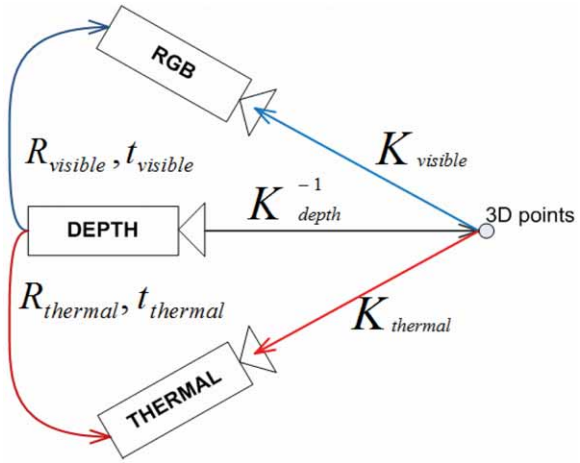

Figure 5. *Stereo calibration of the depth camera with the RGB and thermal cameras.*

In order to calculate the calibration parameters of the cameras, reference points have to be determined. The reference points are selected from a series of images of the same scene, taken by each camera integrated into the 4D thermal imaging system. During the process of calibration of RGB camera, selected reference points are usually the corners of a printed-out checkerboard pattern. Since a printed checkerboard cannot be distinguished by a thermal camera, or the depth camera, alone other approaches have to be applied. Authors in *(23)* used a pattern of black circles placed on white background. In order to make it visible to the thermal camera, they heated the pattern. Different emissivity of the black and white colors caused the pattern to be visible in the thermal image. Instead of directly heating the pattern, it is possible to achieve different emissions of thermal radiation using a white light projector directed at the pattern, as shown in *(5)*. Calibration of a depth and an RGB camera has been addressed in *(16)*, where the checkerboard was placed on top of a table. Since the table was rectangular, its corners were used as the reference points for depth camera calibration.

This paper presents a novel calibration pattern that can be used to determine the corresponding reference points in RGB, thermal and depth images simultaneously. The pattern is composed of rectangular holes cut through a solid board. The board should be made of a thermal insulation material, such as Styrofoam, and preferably should not be too thick to avoid hole occlusion. If the pattern board is too thick, tilting it under a high enough angle relative to the camera would cause that the holes of the board are not completely visible because of the inner edges of the holes. Occluded holes are harder (or impossible) to process in detection of corner reference points. The reason for such a design of the pattern is that it is visible by all the cameras present in the system. Thermal cameras can distinguish the hole pattern due to the thermal radiation emitted by the objects located behind the board and passing through the holes so no additional heating of the board is necessary. Also, the depth image

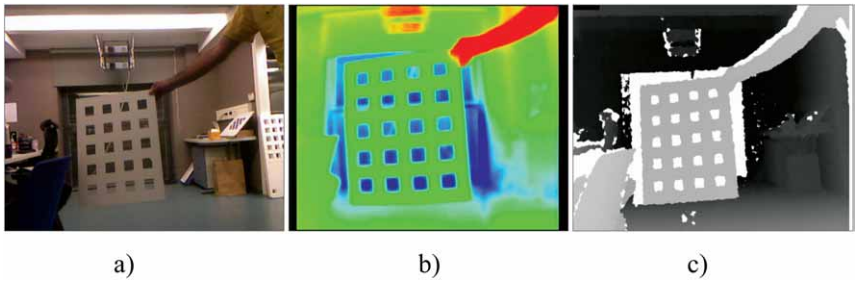

Figure 6. *Novel calibration pattern, as seen by the a) RGB camera, b) thermal imaging camera and c) depth camera.*

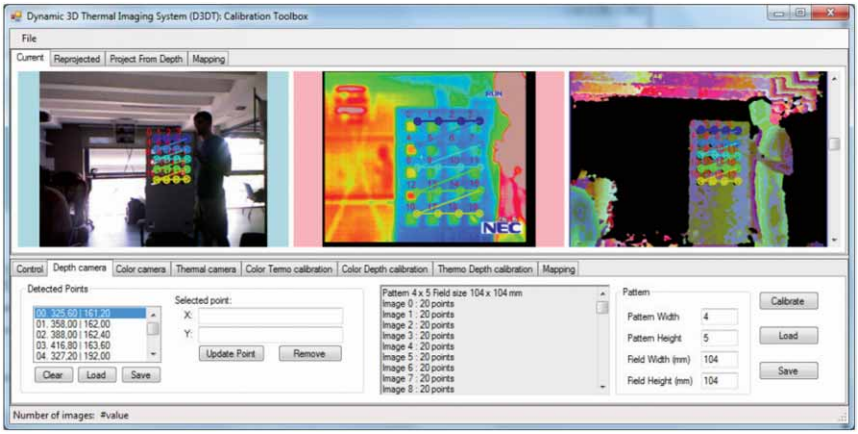

Figure 7. *Graphical User Interface (GUI) design of the system calibration tool.*

results in sharper changes of the depth value in place of the holes, since the depth at those place equals the distance of objects behind the board. As for the RGB camera, it is intuitive that the visible light passes through the holes, thus making them visible in the image.

A novel calibration tool, that incorporates the methodology described in this section, has been constructed. The tool is specially designed to allow easier calibration between multiple imaging modalities by providing simultaneous renderings of the RGB, thermal and depth cameras.

Figure 6 shows the calibration pattern as viewed from the RGB camera, the thermal imaging camera and the depth camera. Figure 7 shows the Graphical User Interface (GUI) of the tool for system calibration developed as par of this project, which employs the methods described in this section.

MOTION CAPTURING AND ANALYSIS

Dynamic monitoring of objects is based on tracking the movement of objects through time. The detection of their motion is most often performed using marker-based techniques where devices called *markers* are placed on the key-points of an object, to enable the measurement of its movement. In human motion detection, one of the most popular techniques uses reflective markers placed on the skin of a subject. Although marker motion detection is precise, popular and simple in concept, this method includes several limitations, such as the preparation time for marker placement, required controlled environment for high quality data acquisition, influence of the attached marker on the subject's movement and others *(24)*. On the other hand, as an alternative, *markerless* motion detection has grown stronger with the development of computer vision technology. Until recently, markerless methods weren't widely available because of the challenges of precise capture of human movement.

Although there are methods for human motion detection and monitoring based on the analysis of consecutive images from a video sequence such as the one based on optical flow described in *(24)*, the task of robust interactive markerless human motion tracking has been greatly simplified by the introduction of real-time depth cameras *(9)*. This study utilized skeletal detection for motion analysis, based on the method described in (9), and implemented in the Kinect device. The algorithm is robust and efficient, and can predict the 3D positions of body joints from a single depth image without any additional temporal information. Authors in *(9)* introduced body part recognition as an intermediate step for human pose estimation. Synthetic data set of highly varied human poses is used to train the classification system, based on very deep decision forests. Simple and depth invariant features were used to train the classifier (without overfitting), learning invariance to pose and shape. The final set of confidence-weighted 3D joint proposals is given by detecting modes in a density function. The results showed a high correlation between real and synthetic data, and the intermediate classification and the final joint proposal

accuracy *(9)*. The accuracy was determined by comparing the estimated position of joints with their reference ground-truth position, which resulted in about 0.9 mAP (mean average precision) *(9)*.

The importance of markerless detection for the system described in this study lies in the application of this system in automatic determination of the temperatures of body parts while a subject performs an exercise. Since thermal cameras and the depth camera are mutually calibrated, the distribution of temperature recorded with a thermal camera can be overlayed accurately on the reconstructed 3D skin surface of the recorded subject. With the localization of the same points in consecutive frames, specifically joint locations of the estimated skeleton, it is possible to extract temperature measurements on the corresponding skin surface above the subjects' joint. If marker-based approach for motion detection was used, parts of the body over and nearby the joints would be occluded by markers, and temperature distribution measurements would not be possible. Temperature values determined at every frame are used to collect statistical data related to the subjects performance, and will be used in further research in an attempt to automatically classify various physiological disorders of the human motor system, skin diseases, cardiovascular disorders or other pathologies detectable through dynamic (or static) temperature measurements and motion analysis. It is important to mention that the performance and accuracy of the joint temperature detection is limited by the accuracy of the skeleton detection algorithm and the associated hardware which is expected to improve in the future.

DISCUSSION ON MEDICAL APPLICATIONS OF 4D THERMAL IMAGING SYSTEM

Acquisition modalities: RGB image, thermal image, depth map and motion capture, of the proposed 4D thermal imaging system, enable real-time capturing of the 3D thermal model of an object. The system combines capabilities of 3D thermography and markerless motion analysis in a variety of medical applications. Those capabilities enable monitoring temperature changes of the human body and characterization of human motion in practical, noninvasive and inexpensive way.

The 3D thermography integrates thermal imaging with 3D geometry to produce standardized 3D thermograms allowing quantitative analysis based not only on temperature distribution but also on shape *(11, 12, 13)*. 3D thermography enables integration of anatomical and physiological information temperature distribution on the skin of the human body. Anatomical information of the whole human body can enhance comparison of temperature patterns in particular regions of the human body. Temperature patterns in both sides of the body are usually symmetrical and any significant asymmetry of more than 0.7°C is a useful indicator of a physiologic or anatomical variant in the loco-motor system *(29, 30)*. In *(31)*, authors showed that the posture variation can cause characteristic temperature patterns in several posture muscles and outlined that this information can be useful for rehabilitation purposes and for preventing pain and other injuries. On the other hand, the temperature distribution of human skin is related to biological and physiological processes that can normally occur or are the result of an illness. This was proved by numerous research studies of medical thermography *(2, 32)*. Thus, integration of structure and temperature information makes 3D thermogram a valuable data model for current and future applications for modeling and simulating biological and physiological processes in the human body *(11, 27)*. In *(12)*, the usage of standardized 3D thermography for quantitative detection of inflammation was proposed. Similar technology was used by authors in *(13)*, as support for monitoring ulcerations and lacerations on diabetic patients affected by Diabetic Foot Disease (DFD). In *(13)* authors used 3D and thermal surface imaging to produce reliable, quantifiable measures of joint volume, shape, and temperature for assessment of disease activity in arthritis.

Analysis of temperature distribution changes over time is especially important when monitoring certain medical states and studying the nature of various dynamic processes in the human body. For example, analysis of temperature changes on certain skin areas during specific physical exercise can provide useful information about thermoregulation mechanism in the human body *(33)* or enhance rehabilitation and preventive programs in sports *(29)*. In *(33)*, authors measured hand skin temperature response under conditions of rest, exercise and recovery from exercise and concluded that thermographic skin response to exercise is characterized by a specific pattern which reflects the dynamic balance between hemodynamic and thermoregulatory processes. Moreover, authors in *(34)* evaluated hand strength of aged subjects by electronic dynamometer complemented with thermographic monitoring, and argued that the method can objectively show the state of the hand motor function of patients with rheumatic arthritis. Furthermore, in *(35)* authors analyzed temperature changes in young and elderly subjects during exercise and presented that both groups have similar capacity for heat production and that elderly subjects have a lower resting temperature and slower heat dissipation. Authors in *(36)* investigate the heat transfer based on the optical flow through a 3D temperature field of a human knee in order to prove diagnostic significance of thermal behavior in determining the pathological status, and propose several therapeutic strategies for the rheumatic knee. Moreover, evaluation of whole body thermal adaptation during physical exercise can help determine ideal conditions for physical activities *(37)*. In *(38)*, authors developed a method for continual measurement of body temperature of moving subjects and outlined the potential of its usage to enhance research on epilepsy and seizures.

The markerless human motion analysis is useful in many different fields concerned with health, such as

kinesiology, orthopedic surgery, physiotherapy, etc. *(39)*. Many pathomechanisms related to musculoskeletal diseases can be diagnosed using motion capturing. Additionally, development and evaluation of various rehabilitative or preventive treatments for the human locomotive system are also possible through motion capturing methods. For this and other similar purposes, serious games are developed and used. Motor rehabilitation through serious games has become an active research during the past few years *(40)*.

The proposed 4D thermal imaging system methodology, that provides various possibilities of modeling and analysis of the human body, can be seen as a valuable part inside the *Virtual Physiological Human* (VPH) framework *(39, 42)*. This framework is based around integrated data model of mechanical, physical and biochemical functions of a living human body. VPH projects are now funded by European Commission as one of the targets in 7th Framework Programme. Many scientific projects related to VPH have been founded by the European Union. One example is the *3D Anatomical Human* project founded in the 6th Framework Programme, with the objective to network a group of researchers from various domains and involve them into modeling and simulation of human body for medical purposes. One of the results is the development of comprehensive methodology to simulate fully subject-specific musculoskeletal models of human articulations built from MRI, motion capture, and body scanning acquisition modalities *(43)*. The general concept behind medical applications of our 4D thermography system can be viewed through generation of the 3D model of the human body complemented with its skin temperature and motion characteristics.

CONCLUSION

This paper presents the development of a 4D thermography system through integration of dynamic 3D thermography and markerless motion analysis. Combining the capabilities of 3D thermography and markerless motion detection enables practical, non-invasive, accurate and automatic monitoring of temperature changes in the human body, and the characterization of human motion. The design of the system based on depth imaging provides a good basis for performing 3D reconstruction of the imaged scene, and is useful for detection of various points of interest, e.g. joint positions of the estimated human skeleton which can be later used for fast and accurate motion tracking and analysis. The thermal imaging, in combination with 3D scene reconstruction, can potentially be used for precise silhouette segmentation, and the separation of an object (or a human subject) from the background. In this case, the dynamically changing point cloud obtained from a person can be used to automatically reconstruct a full 3D human model in real-time. Thus, the proposed system can be valuable for current and future medical applications, for modeling and simulation of biological and physiological processes in human body, as well as for an important potential addition to the concept of the Virtual Physiological Human model. However, some practical limitations of the constructed system are present. Kinect-based 3D scanning currently has lower resolution and precision than some of its existing static 3D imaging alternatives, which prevents accurate 3D reconstruction of smaller objects, or objects with fine-detailed surface. These parameters are also greatly influenced by the distance of the imaged object from the 3D scanner. Also, skeleton detection using Kinect can currently only be performed in the case of full-body scanning. On the other hand, the concept of the system is flexible enough to allow components to be changed or updated, while maintaining the same functionality. For instance, an alternative 3D scanning device might be utilized in place of Kinect to provide greater resolution, precision and accuracy.

The new 4D thermographic technology represents enhanced imaging which provides quantifiable multidimensional and multispectral data sets. The measurement of temperature variation along body surface, provided by multimodal 4D imaging, is becoming a valuable auxiliary tool for the early detection of many medical conditions. Multidimensional and multispectral visualization and the related field of visual analytics are opening the doors towards new interactive medical visualization technologies. Interactive visualization integrated with analysis and reasoning techniques permits new modes of exploration, discovery, reasoning and understanding. 4D thermography has predispositions to improve and define the non-invasive and more economical Health Imaging technology.

Future work should include clinical testing of the presented system on patients with various diagnosed conditions. The collected statistical data can be used to develop new diagnostic methods for the discrimination and classification of disorders based on physiological, vascular and other pathologies.

Acknowledgment: *Authors would like to acknowledge the support of the Croatian Technology Institute and the Technology Transfer Office of the University of Zagreb through the project »4D thermographic system for medical diagnostics«, 4D-TGPOC2_01_14-U-1, 2011.*

REFERENCES

1. VOLLMER M, MÖLLMANN K-P 2010 »Infrared Thermal Imaging: Fundamentals, Research and Applications«, Wiley-VCH Verlag GmbH & Co., Weinheim.
2. DIAKIDES N A, BRONZINO J D 2008 »Medical Infrared Imaging«. Taylor & Francis Group, LLC.
3. MINKINA W, DUDZIK S 2009 »Infrared Thermography Errors and Uncertainties«. John Wiley & Sons, Ltd.
4. KOLARIĆ D, GJENERO L, SKALA K 2010 »Detection of biogas at the municipal waste landfill using a thermal imaging«. Proceedings of the International Scientific congress Energy and Environment, p 449–456
5. KOLARIĆ D, LIPIĆ T, GRUBIŠIĆ I, GJENERO L, SKALA K 2011 »Application of Infrared Thermal Imaging in Blade System Temperature Monitoring«. Proceedings Vol. I. MEET&GVS 34th International Convention MIPRO, p 309–312

6. POLJAK-BLAŽI M, KOLARIĆ D, JAGNJAC M, ŽARKOVIĆ K, SKALA K, ŽARKOVIĆ N 2009 »Specific thermographic changes during Walker 256 carcinoma development: Differential infrared imaging of tumour, inflammation and haematoma«, *Cancer Detection and Prevention 32:* 431–436
7. SANSONI G, TREBESCHI M, DOCCHIO F 2009 »State-of-The--Art and Applications of 3D Imaging Sensors in Industry, Cultural Heritage, Medicine, and Criminal Investigation«. *Sensors 9:* 568–601; doi:10.3390/s90100568
8. WEISS A, HIRSHBERG D, BLACK M J 2011 »Home 3D body scans from noisy image and range data«. To appear: Int. Conf. on Computer Vision, ICCV.
9. SHOTTON J, FITZGIBBON A, COOK M, SHARP T, FINOCCHIO M, MOORE R, KIPMAN A, BLAKE A 2011 »Real-Time Human Pose Recognition in Parts from Single Depth Images«, CVPR.
10. YANG R, CHEN Y 2011 »Design of a 3-D Infrared Imaging System Using Structured Light«. IEEE Transactions on Instrumentation and Measurement.
11. GRUBIŠIĆ I, GJENERO L, LIPIĆ T, SOVIĆ I, SKALA K 2011 »Active 3D scanning based 3D thermography system and medical applications«, MIPRO 2011: Proceedings of the 34th International Convention on Information and Communication Technology, Electronics and Microelectronics, Vol. 1: MEET&GVS, 300-304, 2011, Rijeka, Croatia.
12. JU X, NEBEL C, SIEBERT J P 2004 »3D thermography imaging standardization technique for inflammation diagnosis«, Proc. of SPIE (Photonics Asia 2004). Beijing (China), p 5640–5646
13. BARONE S, PAOLI A, RAZIONALE A V 2006 »A biomedical application combining visible and thermal 3D imaging«, XVIII Congreso Internactional de Ingenieria Grafica, Sitges.
14. ROUGIER C, AUVIENT E, ROUSSEAU J, MIGNOTTE M, MEUNIER J 2011 »Fall detection from depth map video sequences«. Springer-Verlag, Berlin-Heidelberg, ICOST, LNCS 6719, p 121–128
15. ZHANG Z 2000 »A Flexible New Technique for Camera Calibration«. *IEEE Transactions on Pattern Analysis and Machine Intelligence 22(11):* 1330–1334
16. HERRERA C D, KANNALA J, HEIKKILA J 2011 »Accurate and Practical Calibration of a Depth and Color Camera Pair«, CAIP.
17. STONE E E, SKUBIC M 2011 »Evaluation of an Inexpensive Depth Camera for Passive In-Home Fall Risk Assessment«. To appear 5th Int. Conf. on Pervasive Computing Technologies for Healthcare, Dublin, Ireland.
18. GOTTFRIED J-M, FEHR J, GARBE C S 2011 »Computing range flow from multi-modal Kinect data«. Springer-Verlag, Berlin-Heidelberg, ISVC.
19. ZHANG C, ZHANG Z 2011 »Calibration between depth and color sensors for commodity depth cameras«. International Workhsop on Hot Topics in 3D, in conjunction with ICME. Barcelona, Spain.
20. SANDBERG D 2011 »Model-Based Video Coding Using a Colour and Depth Camera«, DICTA11.
21. BOUGUET J-Y 2004 »Camera Calibration Toolbox for Matlab«. Intel Corp, http://www.vision.caltech.edu/bouguetj/calib_doc/
22. HILLMAN P 2005 »White Paper: Camera Calibration and Stereo Vision«. Tech. rep., Square Eyes Software, UK.
23. NEBEL J-C 2003 »3D thermography for quantification of heat generation resulting from inflammation«. Proc. 8th 3D Modelling symposium, Paris, France.
24. CORAZZA S, MÜNDERMANN L, CHAUDHARI A M, DEMATTIO T, COBELLI C, ANDRIACCHI T P 2006 »A Markerless Motion Capture System to Study Musculoskeletal Biomechanics: Visual Hull and Simulated Annealing Approach«. *Annals of Biomedical Engineering 34(6):* 1019–1029
25. PERŠ J, SULIĆ V, KRISTAN M, PERŠE M, POLANEC K, KOVAČIČ S 2010 »Histograms of Optical Flow for Efficient Representation of Body Motion«. *Pattern Recognition Letters 31(11):* 1369–1376
26. BOROJEVIĆ N, KOLARIĆ D, GRAZIO S, GRUBIŠIĆ F, ANTONINI S, NOLA I A, Ž. HERCEG Ž 2011 »Thermography of Rheumatoid Arthritis and Osteoarthritis«. Proceedings of the 53rd International Symposium on Electronics in Marine«, ELMAR.
27. SOVIĆ I, LIPIĆ T, GJENERO L, GRUBIŠIĆ I, SKALA K 2011 »Heat source parameter estimation from scanned 3D thermal models«, MIPRO. Proceedings of the 34th International Convention on Information and Communication Technology, Electronics and Microelectronics, Vol. 1: MEET&GVS, p 283–287. Rijeka, Croatia.
28. SPALDING S J, KWOH C K, BOUDREAU R, ENAMA J, LUNICH J, HUBER D, DENES L, HIRSCH R 2008 »Three dimensional and thermal surface imaging produces reliable measures of joint shape and temperature: a potential tool for quantifying arthritis«. *Arthritis Research & Therapy 10:* R10
29. HILDEBRANDT C, RASCHNER C, KURT AMMER 2010 »An Overview of Recent Application of Medical Infrared Thermography in Sports Medicine in Austria«. Sensors.
30. VARDASCA R 2008 »Symmetry of temperature distribution in the upper and lower extremities«. *Thermol Int 18:* 154–155
31. ABATE M, DI CARLO L, DI ROMUALDO S, IONTA S, FERRETTI A, ROMANI G L, MERLA A 2010 »Postural adjustment in experimental leg length difference evaluated by means of thermal infrared imaging«. *Physiol Meas 31:* 35–43
32. SZENTKUTI A, SKALA KAVANAGH H, GRAZIO S 2011 »Infrared thermography and image analysis for biomedical use«. *Period biol 113(4):* 385–392
33. ZONTAK A, SIDEMAN S, VERBITSKY O, BEYAR R 1998 »Dynamic thermography: analysis of hand temperature during exercise«. *Ann Biomed Eng 26:* 988–993
34. SKALA KAVANAH H, DUBRAVIĆ A, GRAZIO S, LIPIĆ T, SOVIĆ I 2011 »Computer supported thermography monitoring of hand strength evaluation by electronic dynamometer in rheumatoid arthritis – a pilot study«. *Period biol 113(4):* 433–437
35. FERREIRA J J A, MENDONC L C S, NUNES A C C, ANDRADE F, REBELATTO J R, SALVINI T F 2008 »Exercise associated thermographic changes in young and elderly subjects«. *Ann Biomed Eng 36:* 1420–1427
36 XIAO J, HE Z-Z, YANG Y, CHEN B-W, DENG Z-S, LIU J 2011 »Investigation on three-dimensional temperature field of human knee considering anatomical structure. International«. *Journal of Heat and Mass Transfer 54:* 1851–1860
37. MERLA A, MATTEI P A, DI DONATO L, ROMANI G L 2010 »Thermal Imaging of cutaneous temperature modifications in runners during graded exercise«. *Ann Biomed Eng 38:* 158–163
38. BILODEAU G-A, TORABI A, LEVESQUE M, OUELLET C, LANGLOIS J P, LEMA P, CARMANT L 2010 »Body temperature estimation of a moving subject from thermographic images«. *Machine Vision and Applications 56:* 59
39. MÜNDERMANN L, CORAZZA S, CHAUDHARI A M, ANDRIACCHI T P, SUNDARESAN A, CHELLAPPA R 2006 »Measuring human movement for biomechanical applications using markerless motion capture«. IS&T/SPIE 18th Annual Symposium. Electronic Imaging, San Jose, California.
40. SCHÖNAUER C, PINTARICY T, KAUFMANNZ H 2011 »Full Body Interaction for Serious Games in Motor Rehabilitation«. AH '11, Mar 12–14, Tokyo, Japan
41. STEP CONSORTIUM 2007 »Seeding the EuroPhysiome: A Roadmap to the Virtual Physiological Human«, [Online] 5 July 2007, http://www.europhysiome.org/roadmap.
42. MAGNENAT-THALMANN N, ZHANG J. J, FENG D D 2009 »Recent Advances in the 3D Physiological Human«. Springer-Verlag, London Limited
43. MAGNENAT-THALMANN N, SCHMID J, ASSASSI L, VOLINO P 2010 »A comprehensive methodology to visualize articulations for the physiological human«, in Cyberworlds. IEEE Computer Society, p 1–8